Elastic scattering of electrons from positive ions

J. Phys. B: At. Mol. Opt. Phys. **32** (1999) 513–525. Printed in the UK PII: S0953-4075(99)97577-6

Elastic scattering of electrons from positive ions

J T Shepherd and A S Dickinson

Department of Physics, University of Newcastle-upon-Tyne, Newcastle-upon-Tyne, NE1 7RU, UK

Received 15 September 1998

Abstract. Differential cross sections for the elastic scattering of electrons from the ions Na^+, Cs^+, Mg^{2+}, N^{3+} and Ar^{8+} have been calculated employing model- and pseudopotential and quantum-defect methods. Comparison with recent experiments showed satisfactory agreement for Na^+ and N^{3+} but poorer agreement for Cs^+ and Ar^{8+} targets. Generally, model-potential results were in better agreement with experiment than those obtained using pseudopotentials.

1. Introduction

Interest in the field of low energy scattering of electrons from positively charged ions has increased over recent years following experimental advances which have allowed the measurement of differential cross sections for elastic scattering (Bélenger *et al* 1996, Srigengan *et al* 1996a–c, Williams 1997). Several of the targets studied (Na^+, Cs^+, N^{3+}, Ar^{8+}) are closed-shell systems. Here the interaction of the electron with the target can be modelled using a spherically symmetric potential. Information about this potential can also be obtained from the spectroscopy of the composite system of electron + target, e.g. Na. Such information is often presented in the form of a model or a pseudopotential reproducing the energy levels obtained from spectroscopy (Peach 1982). Here we employ such potentials to predict the cross sections for comparison with scattering observations. We also assess whether the potentials giving the best agreement with the spectroscopic observations also give the best agreement with the scattering data. In addition we investigate the extent to which these differential cross sections can be reproduced employing phase shifts inferred from energy levels directly using quantum-defect theory (Seaton 1958).

Section 2 contains a brief review of the relevant scattering theory. The model potentials are introduced in section 3. Section 4 presents the results obtained for various model potentials for a series of positively charged ions. Our conclusions are presented in section 5. Atomic units ($m = \hbar = e = a_0 = 1$) will be used throughout.

2. Scattering theory

2.1. Scattering by a modified Coulomb field

The potentials to be considered are such that

$$V(r) = V_1(r) - Z/r \tag{1}$$

with $V_1(r)$ of short range, that is falling off faster than $1/r^2$, with Z the residual charge of the target ion.

0953-4075/99/020513+13$19.50

We introduce f_1, the non-Coulomb scattering amplitude due to V_1 (Mott and Massey 1965):

$$f_1(k,\theta) = \frac{1}{2ik}\sum_{l=0}^{\infty}(2l+1)e^{2i\sigma_l}(e^{2i\delta_l}-1)P_l(\cos\theta), \tag{2}$$

where k denotes the wavenumber, the σ_l and δ_l are the Coulomb and non-Coulomb phase shifts, respectively, for the angular momentum quantum number l. If f_C denotes the Coulomb scattering amplitude (Mott and Massey 1965),

$$f_C(k,\theta) = \frac{Z}{2k^2\sin^2(\theta/2)}e^{2i\sigma_0}e^{i(Z/k)\ln\sin^2(\theta/2)} \tag{3}$$

where θ is the scattering angle, then the differential cross section is obtained from

$$\frac{d\sigma}{d\Omega} = |f_C(\theta)+f_1(\theta)|^2. \tag{4}$$

2.2. Quantum-defect method

Here we review the relation between the scattering and bound state solutions for potentials of the form of equation (1). The shielding effect of the core electrons surrounding an alkali-like nucleus, represented by $V_1(r)$, modifies the short-range potential experienced by the valence electron and so the energy levels may be written as

$$E_{nl} = -\frac{1}{2}\frac{Z^2}{(n-\mu_{nl})^2} \tag{5}$$

where the μ_{nl} are the quantum defects. These are approximately constant for a given value of l in a particular alkali-like system and so may be written as μ_l.

It has been shown (Seaton 1958) that for all values of l the quantum defects are related to the non-Coulomb phase shifts:

$$\tan\delta_l(k^2) = \frac{\tan\pi\mu_l}{1-e^{-\pi Z/k}}, \tag{6}$$

where the factor $\exp(-\pi Z/k)$ is negligible for most of the cases examined here. This relation gives a convenient way to estimate the non-Coulomb phase shifts, and hence $d\sigma/d\Omega$, from observed energy levels without explicitly introducing the non-Coulomb potential $V_1(r)$.

Using expression (5) quantum defects could be found for relevant ions from energy-level tables. For convenience the values obtained are collected in table 1. For the case of N^{3+} the value of μ_p was not found to be constant over n: this may be attributed to interference from close lying states arising from opening the $2s^2$ subshell. The value of μ_p chosen was that of the $n = 4$ level. For Cs^+ there is an apparent discontinuity between the values of μ_d and of μ_f: we have assumed that the 4f is the lowest f state (Woodgate 1974)—this discontinuity will be discussed further in section 4.2.1.

Table 1. Quantum defects for ion + electron system. The quantum defects for CsI were calculated using values from Moore (1958), and those for other species using the tables of Bashkin and Stoner (1975).

Ion	s	p	d	f	g	h
N^{3+}	0.51	0.27	0.07	0.03	—	—
Na^+	1.36	0.88	0.01	0.001	—	—
Mg^{2+}	1.08	0.72	0.04	0.003	—	—
Ar^{8+}	0.51	0.35	0.09	0.008	—	—
Cs^+	4.06	3.58	2.47	0.03	0.009	0.002

3. Model-potential methods

3.1. Potential forms employed

All the potentials considered here conform to some basic limiting behaviour. Only scattering from ions with filled inner shells has been considered so that spherical symmetry may be assumed and

$$V(r) \longrightarrow \begin{cases} -Z'/r & \text{as } r \to 0 \\ -Z/r & \text{as } r \to \infty \end{cases} \tag{7}$$

where Z' is the charge on the nucleus. Various flexible forms of model potentials and pseudopotentials consistent with (7) have been introduced over the last 60 years. Both model potentials and pseudopotentials are normally optimized to fit the energy levels of the most loosely bound electron. For model potentials the nodal structure of the orbital is preserved, thus for the 3s electron in Na the wavefunction has two nodes. The model potential supports lower-lying states, 1s, 2s and 2p in this case, for which the energies and wavefunctions approximate those from a Hartree–Fock-type calculation. A pseudopotential, on the other hand, is constructed such that its ground state corresponds to the lowest observed state of the system being considered: thus for Na the lowest pseudopotential s-state has no nodes but approximates the observed energy of the 3s state. The absence of lower lying levels offers advantages when performing two-centre, diatomic molecule, calculations employing the pseudopotential, as no avoided crossings with occupied core states can occur. Techniques for refining model potentials obtained from Hartree–Fock (HF) calculations to reproduce observations with spectroscopic precision are discussed by Bartschat (1996). While l-dependent pseudopotentials are also used (Peach 1982), such pseudopotentials are not employed here. Model and pseudopotential methods are discussed in detail by Dixon and Robertson (1978) and by Peach (1982).

Many of the potentials introduced here have been used to model other phenomena, including plasma reaction rates (Bornath *et al* 1994), molecular potentials and non-adiabatic couplings (McCarroll and Valiron 1979, Mó *et al* 1985), molecular potentials for line broadening (Monteiro *et al* 1986) etc.

For these systems a common form of the potential is

$$V(r) = -[(Z' - Z)\Omega(r) + Z]/r \tag{8}$$

where $\Omega(r)$ is known as the screening function. Green *et al* (1969) proposed an independent particle model, which we term the GSZ model, to describe atomic phenomena. The GSZ screening function, $\Omega_G(r)$, is given by

$$\Omega_G(r) = [H(\mathrm{e}^{r/d} - 1) + 1]^{-1} \tag{9}$$

where the parameters H and d were adjusted to fit to experimental data or properties obtained from existing theoretical models. The GSZ parameter values relevant to the ions of interest in this work are collected in table 2.

Another widely used form for the screening function is (Klapisch 1971)

$$\Omega(r) = \sum_{n=0}^{N} q_n r^n \mathrm{e}^{-\alpha_n r} \tag{10}$$

where $q_0 = 1$, $q_n (n \neq 0)$ and α_n are the parameters to be optimized and typically $1 \leqslant N \leqslant 4$. The MAPPAC code of Klapisch (1971) has been used to optimize these parameters for some of the model potentials and pseudopotentials used here and also to obtain the energy levels arising from such potentials and those with $\Omega(r)$ given by equation (9). For this screening function minor modifications to MAPPAC were introduced.

Table 2. The values of the parameters, H and d, of the GSZ screening function, $\Omega_G(r)$. The method of determining the parameters labelled 'I' refers to minimization of the total energy of the system consisting of the valence electron bound to the ionic target (Szydlik *et al* 1974, Szydlik and Green 1974). Method 'II' used a best fit to the valence spectrum of the ion + electron system (Bornath *et al* 1994).

Ion	H	d	Method
Na^+	1.6644	0.5840	I
Na^+	1.337	0.493	II
Cs^+	5.121	1.000	II
N^{3+}	1.3748	0.455	I
Ar^{8+}	1.1616	0.220	I
Mg^{2+}	1.25	0.39	I

Table 3. Phase-shifts in radians for 10 eV electrons (Manson 1969).

Ion	s	p	d	f
Na^+	4.2	2.6	0.2	—
Cs^+	12.0	10.5	7.8	3.2

Table 4. First inelastic thresholds for relevant ions (eV). Values from Bashkin and Stoner (1975), except for Cs^+ from Moore (1958).

Ion	Na^+	Cs^+	N^{3+}	Ar^{8+}	Mg^{2+}
Threshold	33.0	13.3	16.2	252.1	52.4

3.2. HS(HFS) potential

Phase-shifts for the first three partial waves for electron–Na^+ scattering and the first four for electron–Cs^+ collisions for energies up to 27 eV were obtained by Manson (1969) using the unrelaxed Herman–Skillman (Hartree–Fock–Slater) (HS(HFS)) potential, which takes the form

$$V(r) = -\frac{Z'}{r} + \frac{1}{r}\int_0^r \sigma(t)\,\mathrm{d}t + \int_r^\infty \frac{\sigma(t)}{t}\,\mathrm{d}t - 3\left(\frac{3}{8\pi}\rho(r)\right)^{1/3} \tag{11}$$

where $\rho(r) = \sigma(r)/4\pi r^2$ is the spherically averaged total electron charge density. The final term brings in an estimate of the exchange potential. His phase shifts, presented in table 3, have been used in calculations of the differential cross sections for the elastic scattering of electrons from Na^+ and Cs^+ at 10 eV for comparison with other methods.

4. Calculations of differential cross sections

The theory outlined in section 2 is valid only for elastic collisions, so an upper electron energy may be imposed based on the first excitation threshold of the ionic targets: those of interest are listed in table 4.

4.1. Na^+

4.1.1. Potentials and energy levels. Five model potentials and a pseudopotential were introduced and calculations using quantum-defect phase shifts from equation (6) and Manson's phase shifts were also performed. Before considering the scattering results we examine the

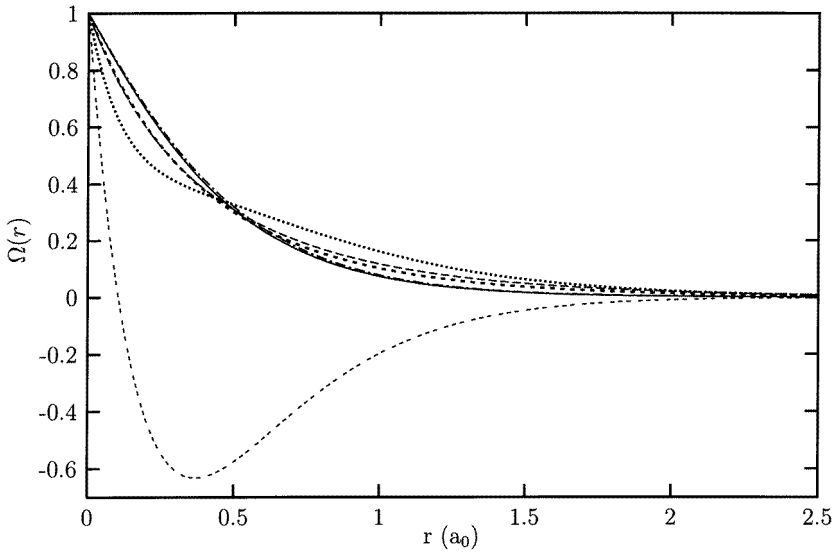

Figure 1. Comparison of model and pseudopotentials for Na^+. Mó *et al* (1985) (—); GSZ(I) Szydlik *et al* (1974) (– – –); GSZ(II) Bornath *et al* (1994) (- - - -); Klapisch (1971) (· · · · · ·); Hanssen *et al* (1979) (— · —); Mendizabal *et al* (1987) (- - - - - -).

accuracy of the various model potentials over the twelve lowest energy levels: the accuracy quoted is the rms percentage deviation from the observed value of each computed level.

The potential of Mó *et al* (1985) has one independent parameter such that $q_1 = \beta$, $\alpha_{0,1} = 2\beta$, where $\beta = 1.83$ was chosen to give the best fit to the 3s and 3p states of Na. The deviation from the observed energy levels was found to be 0.8%.

The GSZ potential was introduced with pairs of parameters determined by both of the methods described in section 3, (see table 2 and equation (9)). The energies due to method I were accurate to 2.2%, while those due to method II were within 0.2%, consistent with the different optimization methods employed in each case.

The model potential developed by Klapisch (1969) has the three parameters $\alpha_0 = 7.902$, $q_1 = 2.351$ and $\alpha_1 = 2.688$, obtained using the MAPPAC code. The accuracy obtained in this case was 0.1%.

Hanssen *et al* (1979) introduced a model with four parameters: $q_1 = 1.967\,697$, $q_2 = 0.237\,331$, $q_3 = 0.037\,170$ and $\alpha_{0-3} = 3.728\,150$. This model gave a slightly poorer fit than the Klapisch potential, being accurate to 1.2%.

The pseudopotential due to Mendizabal *et al* (1987) was again of the form of equations (8) and (10) with parameters $q_1 = -9.613$ and $\alpha_{0,1} = 3.774$. The deviation from the observed energy levels was found to be 0.7%.

These six potentials may conveniently be compared in figure 1 by examining the behaviour of the screening function as a function of the electron–ion distance, r.

Values from the simple one-parameter model of Mó *et al* (1985) and the four-parameter model of Hanssen *et al* (1979) are extremely close over all values of r. Both sets of GSZ parameters give similar screening, as expected. All the potentials are in close agreement at a distance of approximately 0.5 a_0. The curves due to the model potentials are of a similar shape, except for that of Klapisch (1969). This model was constructed with a term to represent the interaction with the 1s shell, demonstrated by the faster fall-off of the screening function

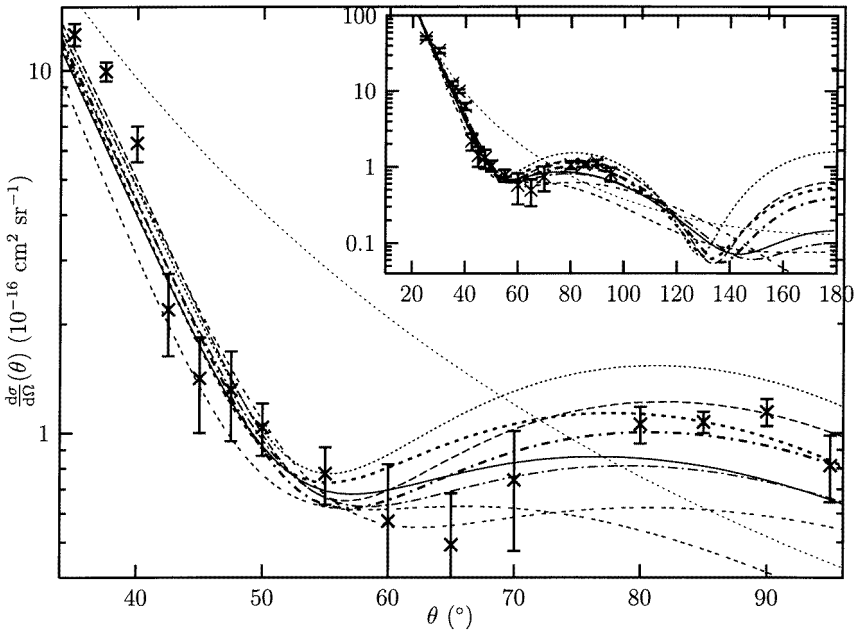

Figure 2. Differential cross sections for the elastic scattering of electrons from Na^+ at 10 eV. Rutherford formula (· · · · · ·). Calculations using the potentials: Mó *et al* (1985) (—); GSZ(I) Szydlik *et al* (1974) (– – –); GSZ(II) Bornath *et al* (1994) (- - - -); Klapisch (1971) (· · · · · ·); Hanssen *et al* (1979) (— · —); Mendizabal *et al* (1987) (- - - - - -); HS(HFS); Manson (1969) (— · —). Quantum defects calculations (- - - - - -). Experimental data: Srigengan *et al* (1996a) (×).

at small r than seen in the other models. This effect was compensated for by the slower fall-off observed at distances 0.4–1.5 a_0. Considering that almost all these model potentials give energies agreeing with experiment within about 1%, the differences seen in figure 1 are relatively large. The shape of the pseudopotential is obviously different to any of the model potentials yet gives comparable outer energy levels.

4.1.2. Differential cross sections. These were determined between 10° and 180°, and are compared in figure 2 with the results of Srigengan *et al* (1996a) for 10 eV electrons. Five partial waves were required to obtain convergence of the results of the model-potential calculations. For the HS(HFS) potential phase shifts were only available for three partial waves, see table 3, so μ_3 was given the value 0.003, corresponding to the appropriate quantum defect, using the approximation $\delta_l \simeq \pi\mu_l$ from equation (6). The quantum defects and HS(HFS) phase shifts for $l > 3$ were set to zero.

On comparing the model-potential methods it may be observed that at most angles the results are bounded by those using the potentials of Klapisch (1969) and of Mó *et al* (1985), as are the screening functions shown in figure 1. Differential cross sections due to the potentials of Mó *et al* (1985) and Hanssen *et al* (1979) remain close over all angles, consistent with the closeness of their screening functions. Good agreement may be seen between all the calculated values and the measured differential cross sections for angles below 55°. However, the observed minimum occurs at an angle around 10° greater than the theoretical predictions suggest and the differential cross section at this minimum is less than any of the calculated

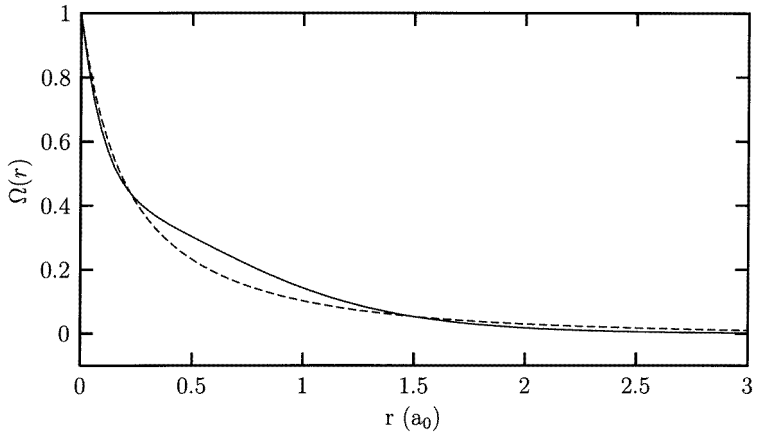

Figure 3. Comparison of model potentials for Cs^+. GSZ(II) Bornath *et al* (1994) (– – –); MAPPAC model (—).

values. A slight maximum was predicted in the region of 80° for the model-potential methods, consistent with the observations. A second minimum was predicted at large angles, 130°–150°, beyond the range of the experiment, by both the model-potential and the quantum-defect calculations. Despite giving excellent bound state energies, the curve due to the pseudopotential of Mendizabal *et al* (1987) gave the poorest agreement with experiment, remaining below the Rutherford result for all angles, displaying a point of inflection close to the first minimum and decreasing further at larger angles.

The Klapisch potential, giving the best fit to the observed energy levels, did not produce the best scattering data for the angles where observations are available. While the differences between the different calculations are not large, apart from those using the pseudopotential, results based on the potential of Bornath *et al* (1994) and the phase shifts of Manson (1969) gave good overall agreement within experimental uncertainty. Considering that the quantum-defect based results employ binding energies of up to ∼5 eV to predict scattering at 10 eV they do surprisingly well, being only slightly worse than the model-potential-based values.

4.2. Cs^+

4.2.1. Potentials and energy levels. Calculations using two model potentials and the quantum-defect approach have been performed. The energy levels due to the GSZ potential were obtained for 11 levels, showing agreement to 6.8%. This is poorer than for the corresponding potential for Na^+, suggesting that the simple two-parameter model may not be adequate to describe such a large and complex ion with four significant quantum defects.

A three-parameter model was developed using the MAPPAC code with $q_1 = 123.812\,97$, $\alpha_0 = 8.037\,57$ and $\alpha_1 = 2.782\,44$ in equation (10). This was optimized to the spectrum of CsI, but a fit could not be obtained with an accuracy better than 14%. In optimizing the parameters it was seen that a potential of the form of equation (10) giving good s, p and d energies was unable to produce good f levels, and vice versa. Increasing the number of parameters in the model did not improve the accuracy. The principal problem was that the 5f, rather than the 4f, level consistent with good s, p and d energies was close to the observed value. It was seen that those potentials giving the best fit to the lower l-value energies gave better scattering results.

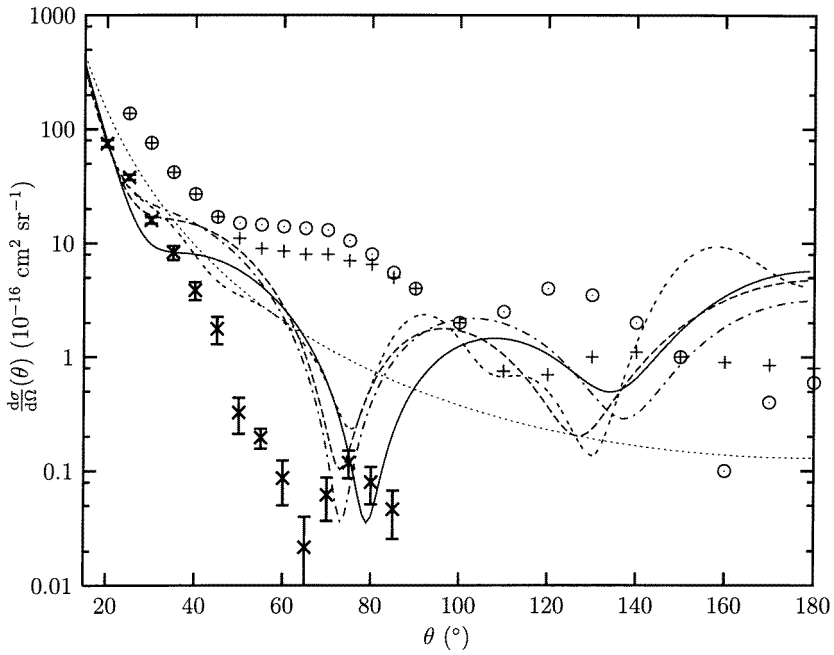

Figure 4. Differential cross sections for the elastic scattering of electrons from Cs^+ at 10 eV. Rutherford formula (· · · · · ·). Calculations using the potentials: GSZ(II) Bornath *et al* (1994) (– – –); MAPPAC model (—); HS(HFS): Manson (1969) (— · —). Quantum defects calculations (- - - - - -). Calculations using HF potential (+), optical potential (⊙) (Johnson and Guet 1994). Experimental data: Srigengan *et al* (1996c) (×).

Comparing the two screening functions, shown in figure 3, significant differences in the region $r \approx 0.6\ a_0$ may be observed.

4.2.2. Differential cross sections. These are compared in figure 4 with the results of Srigengan *et al* (1996b, c) (see also Williams 1997). While experiments were performed at 10, 20 and 30 eV, as the first excitation threshold of Cs^+ is 13.3 eV (see table 4), reliable comparisons could be made only to the 10 eV results. Because all five available theoretical results agreed below 20° and fell below the Rutherford result at 20°, we have normalized the experimental values of Srigengan *et al* (1996b) to our theory at 20°, rather than employing the normalization to the Rutherford value. While this gives improved agreement at small angles, it does not significantly improve the agreement at wider angles.

Qualitative agreement between the results from the model-potential methods and the measurements was observed. For the GSZ potential convergence was only obtained using six partial waves. Manson's phase shifts were used to characterize the HS(HFS) potential for four partial waves, see table 3, and for the higher partial waves the phase shifts were again estimated from the quantum defects.

The model-potential results exceed experiment between 40° and 60° and predict a minimum at angles between 70° and 80°, while the observed value was 65°. The GSZ and HS(HFS) results give similar angular dependences, but differing magnitudes of the differential cross sections. The curve due to the more accurate GSZ bound-state model predicted the minimum closer to that observed.

The relativistic calculations of Johnson and Guet (1994) at 10 eV, with differential cross

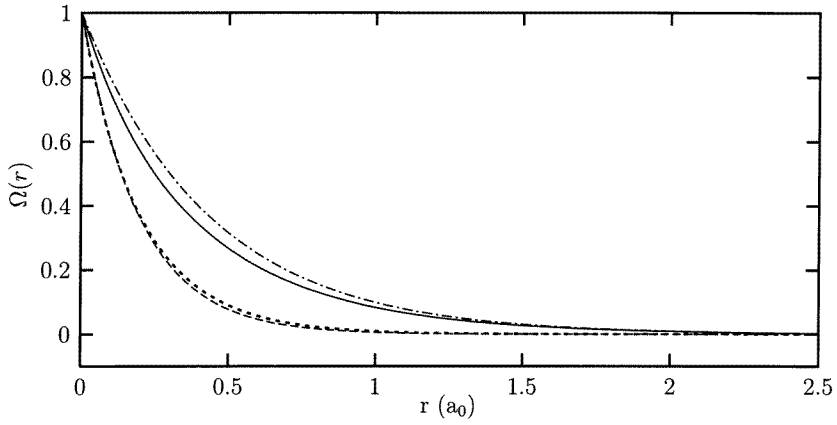

Figure 5. Comparison of model potentials for N^{3+} and Ar^{8+}. N^{3+}: GSZ(I) Szydlik *et al* (1974) (—); McCarroll and Valiron (1979) (— · —). Ar^{8+}: GSZ(I) Szydlik *et al* (1974) (- - - -); MAPPAC model (– – –).

sections remaining above the Rutherford curve for almost all angles, differed substantially from those obtained here. Many-body perturbation theory was used to account for electron correlation using a HF potential and also an optical potential was introduced to model the effect of polarization. The Cs^+ core, being much larger than that in Na^+, has a bigger polarizability: 14.93 au, compared with 0.944 au (Mason and McDaniel 1988). However, these sophisticated calculations gave poorer agreement at 10 eV than the simple, empirical, non-relativistic potential and quantum-defect approaches.

4.3. N^{3+}

4.3.1. Potentials and energy levels. Calculations have also been performed on more highly charged species with filled inner shells, such as N^{3+} ($1s^2 2s^2\ ^1S$), using model-potential and quantum-defect approaches.

The energies obtained from the GSZ potential for this ion deviated from experiment by 3.4% over nine energy levels. A screening function constructed by McCarroll and Valiron (1979) with $q_1 = 0.1152$ and $\alpha_{0,1} = 2.422$ in equation (10) was found to be accurate to 1.5% for these levels. Comparison of the screening functions, shown in figure 5, reveals only small differences.

4.3.2. Differential cross sections. These are compared with experiment (Williams 1997) in figure 6 and can be seen to lie very close to the Rutherford curve for scattering angles less than 60°. Due to the stronger Coulomb forces involved here compared to those for Na^+ discussed above, it is expected that deviations from the Rutherford cross section occur only at angles much larger than in Na^+ and hence larger than the maximum angle, 55°, probed by this experiment. The three sets of results obtained here deviate at angles greater than 80°, showing a deep minimum between 110° and 114°. The similarities between the two model-potential results are consistent with the closeness of their screening functions (see figure 5). Convergence was obtained for five partial waves. Very close agreement may be observed between the quantum-defect method and calculations using the GSZ screening function, where the quantum defects for $l > 3$ were, again, set to zero. Further measurements are desirable to examine scattering beyond 60°.

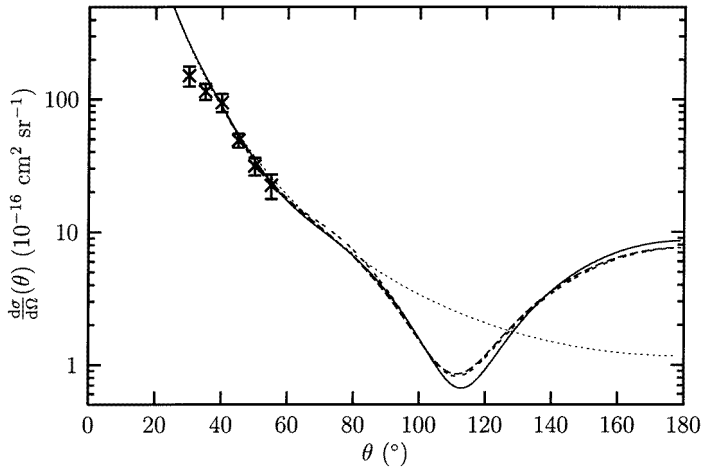

Figure 6. Differential cross sections for the elastic scattering of electrons from N^{3+} at 10 eV. Rutherford formula (· · · · · ·). Calculations using the potentials: GSZ(I) Szydlik *et al* (1974) (– – –); McCarroll and Valiron (1979) (—). Quantum defects calculations (- - - - - -). Experimental data: Williams (1997) (×).

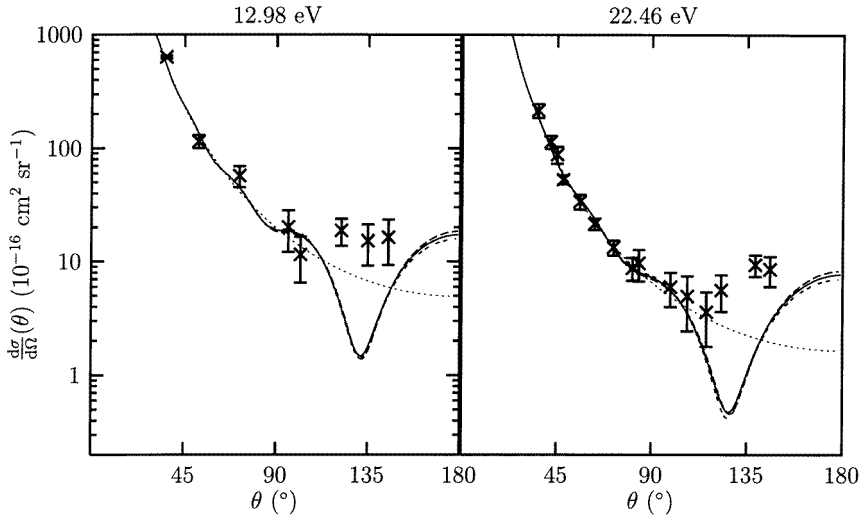

Figure 7. Differential cross sections for the elastic scattering of electrons from Ar^{8+} at 12.98 and 22.46 eV. Rutherford formula (· · · · · ·); Calculations using the potentials: GSZ(I) Szydlik *et al* (1974) (– – –); MAPPAC model (—); Quantum defects calculations (- - - - - -); Experimental data: Bélenger *et al* (1996) (×).

4.4. Ar^{8+}

4.4.1. Potentials and energy levels. Energy levels obtained from the GSZ potential deviated from the observed by 1.0% over 12 levels. A potential with parameters optimized to spectroscopic data was obtained using the MAPPAC code with $q_1 = -0.233\,13$, $\alpha_0 = 5.086\,63$ and $\alpha_1 = 4.480\,94$ in equation (10). This model potential was accurate to 0.4%. In figure 5 it may be seen that these two screening functions are very close over all r.

4.4.2. Differential cross sections. The threshold for excitation of this species is very high, see table 4, so elastic collisions occur for a large range of electron energy. Results from calculations using the two model potentials and the quantum-defect method performed at 12.98 and 22.46 eV are shown in figure 7. Values from the three calculations agreed very closely over all angles, consistent with the closeness of the models and their reproduction of the quantum defects. Convergence of the model-potential methods was obtained for four partial waves.

Measurements of differential cross sections between 35° and 140° at 12.98 and 22.46 eV by Bélenger *et al* (1996) are also shown. These results were normalized to those obtained from scattering from a reference beam, $^3He^{2+}$, with the same beam characteristics and geometry, where the Rutherford expression is valid. They agree with their relativistic HF predictions within experimental uncertainty. None of the calculations or the observations deviated significantly from the Rutherford curve for scattering angles less than 90°. At larger angles all our calculations show a deep minimum at about 130° while experiment shows a plateau between 90° and 140°. These features were well reproduced by the HF calculations. The resolution of the experiment was such that the very weak oscillations about the Rutherford result predicted at angles below 90° were too weak to be observed. These comparisons suggest that relativistic effects are significant in this system and, while they can be mimicked for the energy levels with a non-relativistic local potential, this Hamiltonian fails to reproduce the scattering data.

4.5. Mg^{2+}

4.5.1. Potentials and energy levels. Calculations have been performed for this system using model potentials, a pseudopotential and quantum defects, as experiments are planned (Williams 1998). The GSZ model produced energies accurate to 1.1% over 12 levels. Another model potential with coefficients and exponents found using the MAPPAC code to fit to the two lowest-lying energy levels of Mg^+ was introduced, (Monteiro *et al* 1986), with parameters $q_1 = 2.118$, $q_2 = 1.149$, $\alpha_0 = 5.7720$, $\alpha_1 = 3.3049$ and $\alpha_2 = 20.994$. The energy levels due to this model were found to be accurate to 0.2%. A pseudopotential of the same form, due to García–Madroñal *et al* (1992), was also introduced with parameters $q_1 = -12.44$ and $\alpha_{0,1} = 4.12$. The deviation from observed energy levels was 1.8% in this case. The two screening functions show close agreement but, as with Na^+ (see figure 1), the pseudopotential is qualitatively different.

4.5.2. Differential cross sections. It may be seen in figure 8 that the two model-potential results at 10 eV are very close at all angles, consistent with the closeness of their screening functions. Convergence of the results was obtained for three partial waves. The deep minimum at around 130° was predicted by the three methods, with a shallower minimum at 67° shown in the model-potential calculations. The results due to the pseudopotential remained below the Rutherford curve for all angles and displayed a shoulder in the region of 67°, the minimum of the other calculations, showing similar behaviour to the Na^+ pseudopotential results discussed above.

5. Summary and conclusions

It has been seen that the theory outlined in section 2 can predict the differential cross sections for scattering of electrons from most of the ions examined. In all cases there is general agreement between the model-potential partial-wave analysis and the quantum-defect approaches.

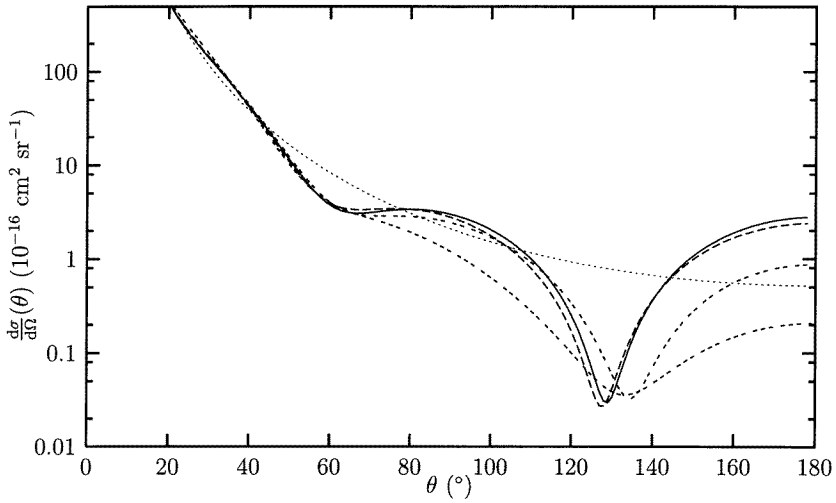

Figure 8. Differential cross sections for the elastic scattering of electrons from Mg^{2+} at 10 eV. Rutherford formula (· · · · · ·); Calculations using the potentials: GSZ(I) Szydlik *et al* (1974) (– – –); Monteiro *et al* (1996) (—); García–Madroñal *et al* (1992) (- - - - - -). Quantum defects calculations (- - - - - -).

The results for scattering from Na^+ show a small but consistent difference from experiment. It was noted that the model potential (Klapisch 1969) giving the best energy-level fit did not produce significantly better scattering results.

The fit for the Cs^+ results showed a similar trend, but the agreement with experiment was poorer than for Na^+. The Cs^+ core is much larger and less tightly bound than that of Na^+, so it may appear that using the same theory as for the smaller ion would be an over-simplification. The relativistic many-body calculations of Johnson and Guet (1994), which explicitly accounted for electron correlation and core polarization, gave a poorer fit than model-potential results at 10 eV.

Model-potential results for N^{3+} agreed with the observations for the limited angular range observed: in this range no significant deviation from the Coulomb result occured so these measurements do not provide a stringent test of the model potentials.

The calculations for Ar^{8+} demonstrated less accord with experiment, however. The HF calculations of Bélenger *et al* (1996) gave differential cross sections agreeing within the experimental uncertainty whereas the simple model-potential and quantum-defect approaches used here did not for angles greater than 100°, the range where significant deviations from the Rutherford result could be seen. These results for Ar^{8+} clearly demonstrate that models capable of reproducing good spectroscopic data will not automatically provide a good description of scattering for highly charged species. Further tests of model-potential methods against differential cross section measurements for highly-charged closed-shell ions would be of interest.

The poor results due to the pseudopotentials in the cases of Na^+ and Mg^{2+} are consistent with the observation (Dixon and Robertson 1978, Peach 1982) that where there is only one outer electron an l-dependent pseudopotential is required rather than the simpler l-independent form used here.

Acknowledgments

This work was supported by the Engineering and Physical Sciences Research Council (UK). We thank Dr I D Williams for supplying tabulated experimental data.

References

Bartschat K 1996 (ed) *Computational Atomic Physics* (Berlin: Springer) p 15
Bashkin S and Stoner J A 1975 *Atomic Energy Levels and Grotrian Diagrams* vols 1 and 2 (Amsterdam: North-Holland)
Bélenger C, Defrance P, Friedlein R, Guet C, Jalabert D, Maurel M, Ristori C, Rocco J C and Huber B A 1996 *J. Phys. B: At. Mol. Opt. Phys.* **29** 4443
Bornath T, Ohde T and Schlanges M 1994 *Physica* A **211** 344
Dixon R N and Robertson I L 1978 *Spec. Period. Rep. Theor. Chem.* **3** 100
García-Madroñal J C, Mó O, Cooper I L and Dickinson A S 1992 *J. Mol. Struct. (Theochem)* **260** 63
Green A E S, Sellin D L and Zachor A S 1969 *Phys. Rev.* **184** 1
Hanssen J, McCarroll R and Valiron P 1979 *J. Phys. B: At. Mol. Phys.* **12** 899
Johnson W R and Guet C 1994 *Phys. Rev.* A **49** 1041
Klapisch M 1969 *PhD Thesis* Université de Paris-Orsay
——1971 *Comput. Phys. Commun.* **2** 239
Manson S T 1969 *Phys. Rev.* **182** 97
Mason E A and McDaniel E W 1988 *Transport Properties of Ions in Gases* (New York: Wiley)
McCarroll R and Valiron P 1979 *Astro. Astrophys.* **78** 177
Mendizabal R, Mó O, Riera A and Yáñez M 1987 *J. Mol. Structure (Theochem.)* **150** 345
Mó O, Riera A and Yáñez M 1985 *Phys. Rev.* A **31** 3977
Moore C E 1958 *United States Department of Commerce National Bureau of Standards Atomic Energy Levels* vol III
Monteiro T S, Cooper I L, Dickinson A S and Lewis E L 1986 *J. Phys. B: At. Mol. Phys.* **19** 4087
Mott N F and Massey H S W 1965 *The Theory of Atomic Collisions* 3rd edn (Oxford: Clarendon)
Peach G 1982 *Commun. At. Mol. Phys.* **11** 101
Seaton M J 1958 *Mon. Not. R. Astron. Soc.* **118** 504
Srigengan B, Williams I D and Newell W R 1996a *Phys. Rev.* A **54** R2540
——1996b *J. Phys. B: At. Mol. Opt. Phys.* **29** L605
——1996c *J. Phys. B: At. Mol. Opt. Phys.* **29** L897
Szydlik P P and Green A E S 1974 *Phys. Rev.* A **9** 1885
Szydlik P P, Kutcher G J and Green A E S 1974 *Phys. Rev.* A **10** 1623
Williams I D 1997 *Invited paper from 20th Int. Conf. Physics of Electronic and Atomic Collisions (Vienna)* p 313
——1998 Private communication
Woodgate G K 1974 *Elementary Atomic Structure* (London: McGraw-Hill)